VIP Shape-Selective Oxidation

DOI: 10.1002/anie.200805342

Shape-Selective Interception by Hydrocarbons of the O_2-Derived Oxidant of a Biomimetic Nonheme Iron Complex**

Anusree Mukherjee, Marlène Martinho, Emile L. Bominaar, Eckard Münck, and Lawrence Que, Jr.**

α-Ketoglutarate-dependent iron enzymes comprise the largest family of dioxygen-activating nonheme iron enzymes that share a common active-site motif.[1] They perform a diverse array of biological functions, including the biosynthesis of collagen, oxygen sensing in cells, DNA and RNA repair, and the demethylation of histones.[2] Dioxygen activation occurs at the iron(II) active site in concert with α-ketoglutarate to generate a high-spin iron(IV) oxo intermediate that effects substrate oxidation.[3–6]

To date, there are only two functional synthetic models for this class of enzymes. In 1995, Valentine and co-workers reported the in situ generation of [Fe(Tp^{Me_2})(BF)],[7] which upon exposure to O_2 carried out the epoxidation of *cis*-stilbene (but not *trans*-stilbene).[8] More recently, Mehn et al. reported the isolation of [Fe(Tp^{Ph_2})(BF)] (**1**) and its crystallographic characterization.[9] Complex **1** reacts with O_2 in benzene at ambient temperature to form in 70% yield green [Fe^{III}(Tp^{Ph_2*})(OBz)] (**2**)[7] that results from oxidative decarboxylation of the BF ligand and the hydroxylation of one of the phenyl rings of the Tp^{Ph_2} ligand (Scheme 1). These examples demonstrate that iron(II) α-keto acid complexes and O_2 react to generate an oxidant, presumably an iron(IV) oxo species by analogy to the enzyme, that can attack olefins and arenes, but there is no example in which C–H bonds are cleaved, which is the principal reactivity exhibited by the α-ketoglutarate-dependent iron enzymes.[2] Herein, we report experiments showing that the oxidant generated in the reaction of **1** with O_2 can be intercepted intermolecularly by hydrocarbons, resulting in the dehydrogenation of the latter. We find that the extent of trapping is governed by both the strength of the C–H bond and the shape of the hydrocarbon. Complex **1** thus serves as a rare example of a simple biomimetic complex with a rudimentary pocket that can discriminate between substrates.

[*] Dr. M. Martinho, Dr. E. L. Bominaar, Prof. Dr. E. Münck
Department of Chemistry
Carnegie Mellon University, Pittsburgh, PA 15213 (USA)
E-mail: emunck@cmu.edu
A. Mukherjee, Prof. Dr. L. Que, Jr.
Department of Chemistry and Center for Metals in Biocatalysis
University of Minnesota, Minneapolis, MN 55455 (USA)
Fax: (+1) 612-624-7029
E-mail: larryque@umn.edu

[**] Research support was provided by the National Institutes of Health (GM-33162 to L.Q.) and the National Science Foundation (MCB-0424494 to E.M. and CHE070073 to E.L.B. through TeraGrid resources provided by the NCSA).

Supporting information for this article is available on the WWW under http://dx.doi.org/10.1002/anie.200805342.

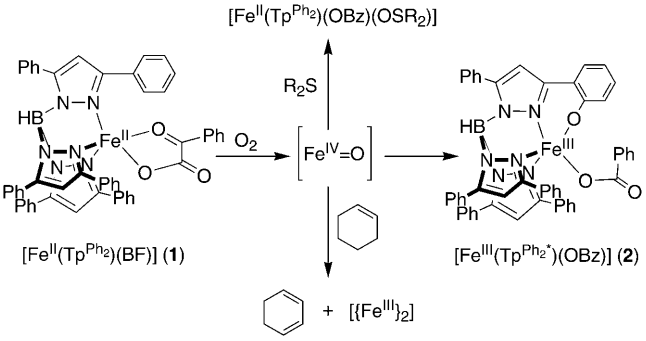

Scheme 1. Reactions of **1** with O_2 in benzene at 25 °C.

Figure 1 shows the UV/Vis spectral changes that accompany the reaction of red-violet **1** with O_2 to form green **2** in about 70% yield.[9] When this reaction was carried out in the presence of thioanisole, the green chromophore was not observed; instead the red-violet chromophore faded to give a colorless solution. Monitoring the reaction by ^{1}H NMR spectroscopy showed the disappearance of paramagnetically shifted features associated with **1** and their replacement by features of [Fe^{II}(Tp^{Ph_2})(OBz)], thus indicating that oxidative decarboxylation occurred. ESI-MS analysis of the resulting solution revealed one prominent peak at *m*/*z* 865.1, corresponding to the [Fe(Tp^{Ph_2})(PhS(O)CH_3)]$^+$ ion. GC analysis found that methyl phenyl sulfoxide was in fact formed in 70% yield, while Mössbauer spectroscopy showed that all of the

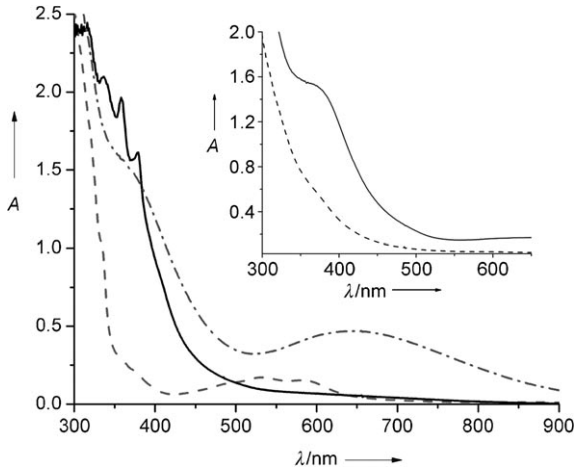

Figure 1. Spectral changes observed in the reactions of **1** (1 mM) with O_2 saturated in benzene at room temperature in a 0.5 cm cell after 1 h. Main plot: – – – **1** alone, –•–• **1** + O_2, —— **1** + O_2 + 0.1 M DHA. Inset: —— **1** + O_2 + 0.1 M cyclohexene, ----- **1** + O_2 + 0.1 M thioanisole.

iron in the oxygenated sample was in the high-spin iron(II) state and that 75% of the iron had an isomer shift and a quadrupole splitting identical to that of a sample derived from the addition of $PhS(O)CH_3$ to $[Fe(Tp^{Ph_2})(OBz)]$ (Figure S1 in the Supporting Information). Addition of one equivalent PhSMe was sufficient to suppress the 650 nm chromophore by 65%, and addition of ten equivalents PhSMe completely prevented its appearance. Thus PhSMe is capable of fully intercepting the oxidant generated in the reaction of **1** with O_2 and preventing the intramolecular hydroxylation of a ligand phenyl group.

We note that the addition of thioanisole did not significantly affect the one hour reaction time required for the disappearance of the iron(II) chromophore. This observation is consistent with the rate-determining step for the oxygenation occurring prior to the interception step, as demonstrated by earlier kinetic studies that showed first-order dependence on both iron complex and O_2.[9] In fact, the rate-determining step likely leads to the formation of the putative Fe^{IV}=O oxidant, so the relative amounts of **2** and interception product observed would then reflect the relative rates of intramolecular and intermolecular interception of the oxidant.

We then investigated whether hydrocarbons could also intercept this oxidant. Figure 1 shows the UV/Vis spectra of the reaction of **1** with O_2 in the presence of 0.1M DHA.[7] Anthracene was formed as a product, as indicated by the appearance of its three characteristic sharp peaks at 379, 357, and 339 nm after a period of one hour. UV quantification after removal of iron showed an anthracene yield of 35%, while the residual absorbance at 650 nm suggested that **2** was formed at only 20% of its original level. Similar results were obtained with 0.1M cyclohexene, where the amount of **2** formed decreased by a factor of four. Cyclohexadiene was obtained in 40% yield, and neither 2-cyclohexenol nor 2-cyclohexenone was observed. Thus, under these conditions, DHA and cyclohexene are capable of intercepting about 75–80% of the oxidant responsible for the self-hydroxylation reaction.

Scheme 2 shows that other hydrocarbons are also capable of intercepting the O_2-derived oxidant. Besides DHA and cyclohexene, cyclopentane and cyclooctane also reacted with the Fe=O oxidant, but their trapping efficiency was significantly lower, probably owing to their stronger C–H bonds. On the other hand, cyclohexane did not affect the ligand hydroxylation at all. The 99.3 kcal mol^{-1} C–H bonds of cyclohexane may represent the upper limit for C–H bonds that can be attacked by the Fe=O oxidant, in agreement with the established reactivity exhibited by the α-ketoglutarate-dependent iron enzymes.

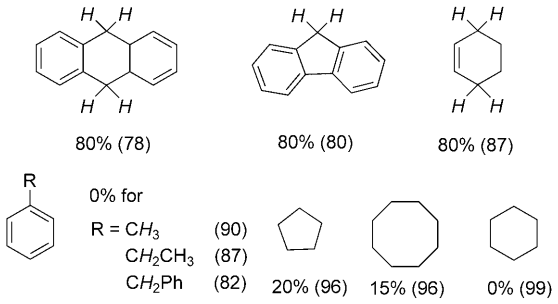

Scheme 2. Hydrocarbon substrates used to intercept the putative Fe^{IV}=O oxidant. Percent values indicate the extent to which the abundance of the green chromophore is decreased in the presence of 0.1 M substrate; values in parentheses are the bond dissociation energies (in kcal mol^{-1}) for the weakest C–H bond in each molecule (to the italicized hydrogen atoms).[10]

Interestingly, toluene, ethylbenzene, and diphenylmethane did not intercept the oxidant at all at the 0.1M concentrations used for these trapping experiments, despite the fact that their C–H bonds have bond strengths comparable to those of cyclohexene. The contrasting behavior of diphenylmethane and fluorene is particularly illustrative. These results suggest that trapping efficiency is modulated not just by the strength of the target C–H bond but also by the accessibility of the substrate to the nascent Fe=O oxidant.

Further corroboration of the above notions comes from the concentration dependences of oxidant trapping, as illustrated in Figure 2a. PhSMe (blue bars) intercepted the oxidant even at a concentration equivalent to that of **1** (1 mM), but isosteric PhEt (indigo bars) required a 1000-fold higher concentration to have the same effect. This difference likely reflects the greater thermodynamic driving force for sulfoxidation than for H-atom abstraction. On the other hand, a similar concentration difference was found for the trapping of the oxidant by cyclohexene (red bars) and PhEt, despite the fact that the two have similar C–H bond strengths. Indeed, a competitive oxidation of cyclohexene and PhEt, both at 0.1M concentration, yielded only cyclohexadiene as the oxidation product. Moreover, cyclohexene at 1 or 10 mM is able to trap the oxidant while DHA is not; at 0.1M concentration, however, both intercept the oxidant with comparable effectivity. These differences suggest that the allylic C–H bonds of cyclohexene have more facile access to the Fe=O "active site" than the benzylic C–H bonds of either ethylbenzene or DHA. This access is controlled by the gap between the two phenyl rings that flank the putative Fe=O unit and favor molecules with an oblate spheroidal shape.

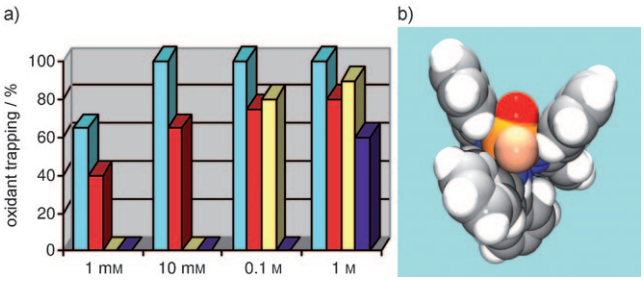

Figure 2. a) Substrate concentration dependence on the percent trapping of the oxidant formed by the reaction of **1** and O_2 in benzene at 25°C. Legend for each data cluster from left to right: thioanisole (blue), cyclohexene (red), DHA (yellow), ethylbenzene (indigo). b) Space-filling representation of the shape-selective cleft flanking the putative Fe^{IV}=O oxidant based on DFT calculations. O(oxo) red, O(carboxylate) pink, Fe gold, N blue, C gray, H white.

Figure 2b shows a representation of the hypothetical Fe^{IV}=O oxidant in which two of the three 3-phenyl groups of the Tp^{Ph_2} ligand form a rudimentary cleft that may serve to

discriminate among various hydrocarbons on the basis of shape. This picture derives from a DFT calculation of the $[Fe^{IV}(O)(Tp^{Ph_2})(OBz)]$ intermediate proposed to carry out the oxidations. Our computations show that the energy for the $S=2$ isomer is lower than for the $S=1$ isomer by 6.2 kcal mol^{-1} (S represents the electronic spin state). Although this energy difference is usually deemed to be greater than the inherent uncertainty of current DFT calculations,[11] its interpretation is complicated by the fact that the two geometry-optimized structures differ in coordination number. We find the $S=1$ isomer to be six-coordinate and the $S=2$ isomer to be five-coordinate owing to a change in the coordination mode of one carboxylate ligand from bidentate to monodentate. Thus the calculated energy difference reflects not only the change in the spin state but also the change in carboxylate binding mode. We postulate that this geometry difference derives from steric crowding of the phenyl groups around the Fe=O unit to afford the lower coordination number for the $S=2$ isomer. In support, calculations for a truncated model containing only one phenyl group showed that both $S=2$ and $S=1$ isomers have six-coordinate Fe^{IV} centers, in agreement with the results reported by Borowski et al.[12] Further details of the calculations are presented in the Supporting Information. Notably, our computed $S=2$ structure resembles that calculated for the high-spin Fe^{IV}=O intermediate of the enzyme TauD.[7,13] Whichever the spin state of the Fe=O species, it is clear from the experimental data that it must be an oxidant powerful enough to cleave the 96 kcal mol^{-1} C–H bonds of cyclopentane and cyclooctane within the one hour time frame of the reaction of **1** and O_2.

Several mechanistic points deserve comment. First, experiments with $[D_{10}]$cyclohexene showed that C–H bond cleavage is a key step in substrate oxidation, even though it is not the rate-determining step for the overall reaction of **1** with O_2. While the oxidation rate of **1** was not affected by the presence of either 0.1 M cyclohexene or $[D_{10}]$cyclohexene, a product isotope effect of 10 was manifested in a competitive oxidation of cyclohexene and $[D_{10}]$cyclohexene. This value is somewhat larger than the classical limit associated with C–H bond cleavage. It is comparable to the kinetic isotope effect found for $[Fe^{IV}(O)(TMC)(NCCH_3)]^{2+}$ [7] in DHA oxidation[14] but is much lower than the values of 30–50 found for $[Fe^{IV}(O)(N4Py)]^{2+}$ [7] in ethylbenzene oxidation[15] and for TauD in the hydroxylation of taurine.[4]

Secondly, we note that cyclohexene was oxidized only to cyclohexadiene. No allylic oxidation products were found, despite the fact that they are commonly observed in aerobic cyclohexene oxidations, owing to trapping of the incipient cyclohexenyl radical by O_2.[16] Their absence strongly suggests that cyclohexenyl radical, the presumed initial product from the attack of the Fe=O oxidant, does not react with the excess O_2 in the reaction solution and must instead be further oxidized more rapidly by the nascent Fe^{III}–OH species to afford the dehydrogenated product. The behavior of this Fe=O species differs from that of $[Fe^{IV}(O)(N4Py)]^{2+}$ in its reaction with hydrocarbons, in which the alkyl radical initially formed by H-atom abstraction is readily trapped by O_2 to afford products of autoxidation.[15]

Thirdly, the observed dehydrogenation of cyclohexene would require the putative Fe^{IV}=O oxidant to be reduced to the Fe^{II} oxidation state, as in the thioanisole oxidation reaction. If this were the case, cyclohexadiene should have been formed in comparable yield to methyl phenyl sulfoxide, not a factor of two less. However, a comparison of the UV/Vis spectra of the two solutions at the end of their respective reactions (Figure 1 inset) suggests a difference in the nature of the iron products. The featureless spectrum of the thioanisole solution is consistent with formation of $[Fe^{II}(Tp^{Ph_2})(OBz)(OSR_2)]$ described earlier, while the strong absorbance near 350 nm observed in the cyclohexene solution suggests formation of an iron(III) byproduct. The latter was confirmed by Mössbauer spectroscopy, which showed that 70% of the iron in the sample belongs to antiferromagnetically coupled diiron(III) centers (Figures S2 and S3 in the Supporting Information). This 350 nm band was observed in all our hydrocarbon oxidation studies except in the case of DHA oxidation, where it was obscured by the sharp peaks of anthracene. The consistent observation of the 350 nm band in the hydrocarbon interception reactions further suggests that they all follow the same route and give rise to the same diiron(III) product. Thus, the Fe^{IV}=O unit in the hydrocarbon oxidations acts effectively as a one-electron oxidant. We suggest that the diiron(III) complex arises from the comproportionation of the initial $[Fe^{II}(Tp^{Ph_2})(OBz)]$ product with the Fe^{IV}=O oxidant as it is formed. Indeed the reaction of **1** with O_2 in the presence of an equimolar amount of $[Fe^{II}(Tp^{Ph_2})(OBz)]$ shows no self-hydroxylation of the ligand phenyl ring and instead affords the diiron(III) byproduct. We attribute the different outcome in the thioanisole experiment to the likelihood that the sulfoxide formed remains coordinated to the iron(II) center, inhibiting the comproportionation.

Lastly, it is significant that cyclohexene is converted to cyclohexadiene rather than 2-cyclohexenol. To date, oxidation of hydrocarbons by biomimetic iron oxo species has generally resulted in hydroxylation rather than dehydrogenation.[15,17] In various metalloenzymes, substrate hydroxylation and dehydrogenation are in fact related transformations that are controlled by the interactions of the substrate with the active-site pocket.[18] DFT calculations indicate that the outcome of the C–H bond oxidation depends on what happens after the rate-determining C–H bond cleavage step.[19] Oxygen rebound from the iron center to the incipient alkyl radical generates the alcohol, while oxidation of the alkyl radical to a carbocation leads to dehydrogenation. The distance between the alkyl radical and the Fe–OH unit is the key factor that controls the outcome; the greater the distance, the less favored is the rebound step. The experimental data clearly show that oxygen rebound does not occur in the oxidation of hydrocarbons in the reaction of **1** with O_2.

In conclusion, we have demonstrated the intermolecular interception of the oxidant formed by oxygenation of the biomimetic iron(II) α-ketocarboxylate complex **1**. The oxidant that is generated not only can cleave fairly strong aliphatic C–H bonds but does so with some shape selectivity. Shape selectivity is rare among biomimetic oxidation catalysts; the best examples are the so-called "picnic basket" metalloporphyrins developed by Collman et al.,[20a] the den-

drimeric metalloporphyrin catalyst designed by Suslick and co-workers,[20b] and the [$Fe^{II}(Tp^{Me_2})(BF)$] complex of Valentine and co-workers mentioned earlier,[8] all of which carry out shape-selective olefin epoxidation. The model complex described herein represents the first example that generates a shape-selective O_2-derived oxidant that cleaves aliphatic C–H bonds and carries out the dehydrogenation of hydrocarbons.

Received: November 1, 2008
Published online: January 29, 2009

Keywords: bioinorganic chemistry · biomimetic reactivity · iron · oxygen activation · shape selectivity

[1] M. Costas, M. P. Mehn, M. P. Jensen, L. Que, Jr., *Chem. Rev.* **2004**, *104*, 939.
[2] R. P. Hausinger, *Crit. Rev. Biochem. Mol. Biol.* **2004**, *39*, 21.
[3] C. Krebs, D. G. Fujimori, C. T. Walsh, J. M. Bollinger, Jr., *Acc. Chem. Res.* **2007**, *40*, 484.
[4] J. C. Price, E. W. Barr, T. E. Glass, C. Krebs, J. M. Bollinger, Jr., *J. Am. Chem. Soc.* **2003**, *125*, 13008.
[5] L. M. Hoffart, E. W. Barr, R. B. Guyer, J. M. Bollinger, Jr., C. Krebs, *Proc. Natl. Acad. Sci. USA* **2006**, *103*, 14738.
[6] D. P. Galonic, E. W. Barr, C. T. Walsh, J. M. Bollinger, Jr., C. Krebs, *Nat. Chem. Biol.* **2007**, *3*, 113.
[7] Abbreviations used: BF = benzoylformate, DHA = 9,10-dihydroanthracene, N4Py = *N*,*N*-bis(2-pyridylmethyl)bis(2-pyridyl)-methylamine, OBz = benzoate, TauD = taurine:α-ketoglutarate dioxygenase, TMC = 1,4,8,11-tetramethylcyclam, Tp^{Me_2} = hydrotris(3,5-dimethylpyrazol-1-yl)borate, Tp^{Ph_2} = hydrotris(3,5-diphenylpyrazol-1-yl)borate.
[8] E. H. Ha, R. Y. N. Ho, J. F. Kesiel, J. S. Valentine, *Inorg. Chem.* **1995**, *34*, 2265.
[9] M. P. Mehn, K. Fujisawa, E. L. Hegg, L. Que, Jr., *J. Am. Chem. Soc.* **2003**, *125*, 7828.
[10] a) Y.-R. Lu, *Comprehensive Handbook of Chemical Bond Energies*, CRC, Taylor & Francis Group, Boca Raton FL, **2007**, chap. 3, p. 19; b) J. R. Bryant, J. M. Mayer, *J. Am. Chem. Soc.* **2003**, *125*, 10351; c) C. R. Goldsmith, R. T. Jonas, D. P. Stack, *J. Am. Chem. Soc.* **2002**, *124*, 83.
[11] a) D. Young, *Computational Chemistry, A practical guide for applying techniques to real world problems*, Wiley Interscience, New York, **2001**, chap. 16, p. 135; b) F. Neese, *J. Biol. Inorg. Chem.* **2006**, *11*, 702.
[12] T. Borowski, A. Bassan, P. E. M. Siegbahn, *Inorg. Chem.* **2004**, *43*, 3277.
[13] S. Sinnecker, N. Svensen, E. W. Barr, S. Ye, J. M. Bollinger, Jr., F. Neese, C. Krebs, *J. Am. Chem. Soc.* **2007**, *129*, 6168.
[14] C. V. Sastri, J. Lee, K. Oh, Y. J. Lee, J. Lee, T. A. Jackson, K. Ray, H. Hirao, W. Shin, J. A. Halfen, J. Kim, L. Que, Jr., S. Shaik, W. Nam, *Proc. Natl. Acad. Sci. USA* **2007**, *104*, 19181.
[15] a) J. Kaizer, E. J. Klinker, N. Y. Oh, J.-U. Rohde, W. J. Song, A. Stubna, J. Kim, E. Münck, W. Nam, L. Que, Jr., *J. Am. Chem. Soc.* **2004**, *126*, 472; b) E. J. Klinker, Ph.D. thesis, University of Minnesota **2007**.
[16] A. Bottcher, M. W. Grinstaff, J. A. Labinger, H. B. Gray, *J. Mol. Catal. A* **1996**, *113*, 191.
[17] a) K. Chen, L. Que, Jr., *J. Am. Chem. Soc.* **2001**, *123*, 6327; b) A. Company, L. Gomez, M. Guell, X. Ribas, J. M. Luis, L. Que, Jr., M. Costas, *J. Am. Chem. Soc.* **2007**, *129*, 15766; c) M. S. Chen, M. C. White, *Science* **2007**, *318*, 783.
[18] a) J. S. Kartha, K. W. Skordos, H. Sun, C. Hall, L. M. Easterwood, C. A. Reilly, E. F. Johnson, G. S. Yost, *Biochemistry* **2008**, *47*, 9756; b) Y. Jin, J. D. Lipscomb, *J. Biol. Inorg. Chem.* **2001**, *6*, 717; c) P. Broun, J. Shanklin, E. Whittle, C. Somerville, *Science* **1998**, *282*, 1315; d) E. Whittle, A. E. Tremblay, P. Buist, J. Shanklin, *Proc. Natl. Acad. Sci. USA* **2008**, *105*, 14738; e) J. E. Baldwin, R. M. Adlington, N. P. Crouch, C. J. Schofield, N. J. Turner, R. T. Aplin, *Tetrahedron* **1991**, *47*, 9881.
[19] D. Kumar, S. P. de Visser, S. Shaik, *J. Am. Chem. Soc.* **2004**, *126*, 5072.
[20] a) J. P. Collman, X. Zhang, V. J. Lee, E. S. Uffelman, J. I. Brauman, *Science* **1993**, *261*, 1404; b) P. Bhyrappa, J. K. Young, J. S. Moore, K. S. Suslick, *J. Am. Chem. Soc.* **1996**, *118*, 5708.

